0026-895X/10/7704-497–507$20.00
MOLECULAR PHARMACOLOGY
Copyright © 2010 The American Society for Pharmacology and Experimental Therapeutics
Mol Pharmacol 77:497–507, 2010

Vol. 77, No. 4
61929/3568651
Printed in U.S.A.

Dominant-Negative Regulation of Cell Surface Expression by a Pentapeptide Motif at the Extreme COOH Terminus of an Slo1 Calcium-Activated Potassium Channel Splice Variant

Yu-Hsin Chiu, Claudia Alvarez-Baron, Eun Young Kim, and Stuart E. Dryer

Department of Biology and Biochemistry, University of Houston, Houston, Texas

Received October 24, 2009; accepted January 4, 2010

ABSTRACT

Large-conductance Ca^{2+}-activated K^+ (BK_{Ca}) channels regulate the physiology of many cell types. A single vertebrate gene variously known as *Slo1*, *KCa1.1*, or *KCNMA1* encodes the pore-forming subunits of BK_{Ca} channel but is expressed in a potentially very large number of alternative splice variants. Two splice variants of Slo1, $Slo1_{VEDEC}$ and $Slo1_{QEERL}$, which differ at the extreme COOH terminus, show markedly different steady-state expression levels on the cell surface. Here we show that $Slo1_{VEDEC}$ and $Slo1_{QEERL}$ can reciprocally coimmunoprecipitate, indicating that they form heteromeric complexes. Moreover, coexpression of even small amounts of $Slo1_{VEDEC}$ markedly reduces surface expression of $Slo1_{QEERL}$ and total Slo1 as indicated by cell-surface biotinylation assays. The effects of $Slo1_{VEDEC}$ on steady-state surface expression can be attributed primarily to the last five residues of the protein based on surface expression of motif-swapped constructs of Slo1 in human embryonic kidney (HEK) 293T cells. In addition, the presence of the VEDEC motif at the COOH terminus of Slo1 channels is sufficient to confer a dominant-negative effect on cell surface expression of itself or other types of Slo1 subunits. Treating cells with short peptides containing the VEDEC motif increased surface expression of $Slo1_{VEDEC}$ channels transiently expressed in HEK293T cells and increased current through endogenous BK_{Ca} channels in mouse podocytes. $Slo1_{VEDEC}$ and $Slo1_{QEERL}$ channels are removed from the HEK293T cell surface with similar kinetics and to a similar extent, which suggests that the inhibitory effect of the VEDEC motif is exerted primarily on forward trafficking into the plasma membrane.

The pore-forming subunits of large-conductance Ca^{2+}-activated potassium (BK_{Ca}) channels are encoded by a conserved vertebrate gene called *Slo1* (also known as *KCNMA1* and *KCa1.1*) (Beisel et al., 2007). This gene encodes proteins with seven transmembrane domains (S0–S6), an ectofacial NH_2 terminus, and a large intracellular COOH terminus (Lu et al., 2006). A tetramer of Slo1 proteins can comprise a functional BK_{Ca} channel (Shen et al., 1994). The physiological importance of BK_{Ca} channels is underscored by the wide range of defects that occur when *Slo1* is knocked out (Meredith et al., 2004; Rüttiger et al., 2004; Sausbier et al., 2004) or after in vivo pharmacological blockade (Imlach et al., 2008).

The vertebrate *Slo1* gene has a conserved intron-exon structure, including at least 35 exons and no fewer than 7 sites in which alternative pre-mRNA splicing can occur (Beisel et al., 2007). The majority of alternative splice sites occur in the large cytosolic COOH-terminal domain, which comprises nearly half of each Slo1 subunit. Some of these variants have been analyzed and have been shown to encode channels with markedly different gating properties and susceptibility to post-translational modulation (Butler et al., 1993; Tseng-Crank et al., 1994; Xie and McCobb, 1998; Shipston, 2001; Wang et al., 2003), such as the five Slo1 variants that differ at splice site 4 (Chen et al., 2005). Alternative splicing at site 7 as defined by Beisel et al. (2007) can result in three different extreme COOH-terminal variants of Slo1 that are found across a wide range of vertebrate species. These include a long form known as $Slo1_{VEDEC}$, and two shorter forms known as $Slo1_{EMVYR}$ and $Slo1_{QEERL}$ (Kim et al., 2007b,c, 2008; Ma et al., 2007; Pietrzykowski et al., 2008) after the last five residues in each isoform. Heterologous expression of these three COOH-terminal variants results in BK_{Ca} channels that have similar gating properties but mark-

This work was supported by the National Institutes of Health National Institute of Diabetes and Digestive and Kidney Diseases [Grant R01-DK82529].
Article, publication date, and citation information can be found at http://molpharm.aspetjournals.org.
doi:10.1124/mol.109.061929.

ABBREVIATIONS: BK_{Ca}, large-conductance Ca^{2+}-activated K^+ channels; HA, hemagglutinin; PDZ, PSD-95/Disks Large/Zonula Occludins; Slo1, pore-forming subunit of large-conductance Ca^{2+}-activated K^+ channels; BSA, bovine serum albumin; HRP, horseradish peroxidase; PBS, phosphate-buffered saline; PCR, polymerase chain reaction; HEK, human embryonic kidney; HEDTA, *N*-(2-hydroxyethyl)-EDTA; R-PE, *R*-phycoerythrin; OD, optical density.

edly different patterns of expression on the cell surface (Kim et al., 2007b; Ma et al., 2007; Ridgway et al., 2009). All three of these variants contain an endoplasmic reticulum export signal described previously (Kwon and Guggino, 2004), whereas none of the ones studied contain a CVLF motif reported to suppress the surface expression of a subset of rat Slo1 splice variants (Zarei et al., 2004). It is noteworthy that $Slo1_{QEERL}$ and $Slo1_{EMVYR}$ show much higher constitutive steady-state expression on the cell surface than $Slo1_{VEDEC}$ (Kim et al., 2007b; Ma et al., 2007; Ridgway et al., 2009). However, the surface expression of $Slo1_{VEDEC}$ approaches that of $Slo1_{QEERL}$ and $Slo1_{EMVYR}$ if cells are stimulated by appropriate growth factors (Kim et al., 2007b). In this study we focus on the $Slo1_{VEDEC}$ and $Slo1_{QEERL}$ variants because they have been shown to coexist in different types of cells and tissues under normal conditions (Beisel et al., 2007; Kim et al., 2007b, 2008).

We demonstrated previously that the coexpression of a soluble fusion protein containing 42 of the unique COOH-terminal residues at the end of $Slo1_{VEDEC}$ increased the surface expression of full-length $Slo1_{VEDEC}$ but had no effect on the surface expression of full-length $Slo1_{QEERL}$ (Kim et al., 2007b). By contrast, coexpression of a fusion protein containing the unique COOH-terminal residues of $Slo1_{QEERL}$ did not produce significant effects on the surface expression of either $Slo1_{VEDEC}$ or $Slo1_{QEERL}$ (Kim et al., 2007b). These data suggest that a motif (or motifs) somewhere in the unique COOH-terminal tail of $Slo1_{VEDEC}$ can suppress constitutive surface expression of Slo1 proteins, but they provide no indication of where within the tail these motifs might be located. Ma et al. (2007) showed that progressive deletions of the unique portions of the $Slo1_{VEDEC}$ COOH-terminal tail led to progressively greater surface expression of the remainder of $Slo1_{VEDEC}$. From this, they concluded that the entire COOH-terminal tail of $Slo1_{VEDEC}$ is important for its retention in intracellular compartments. However, this experimental design cannot exclude that progressive deletions cause increasingly severe disruptions of tertiary structure that affect Slo1 affinity for interactions with other proteins. In addition, deletions could cause motifs to be exposed that might normally be hidden in full-length proteins.

On the other hand, there is substantial literature indicating that sequences as short as four to five residues at the extreme COOH termini of proteins can contribute to functionally significant protein-protein interactions, especially interactions with PSD-95/Disks Large/Zonula Occludins (PDZ) domains. Consistent with this, we have reported recently that the $Slo1_{VEDEC}$ isoforms can bind to proteins that do not interact with the other Slo1 splice variants (Kim et al., 2008) and that Slo1 proteins can interact with the PDZ domains of certain scaffolding proteins that regulate their trafficking (Ridgway et al., 2009). Based on these observations, we hypothesized that the differences in surface expression of Slo1 splice variants could reside in the last few residues of each variant. The purpose of the present study was to test this hypothesis.

Materials and Methods

Plasmid Constructs. Expression plasmids encoding NH_2-terminal Myc-tagged $Slo1_{VEDEC}$ and $Slo1_{QEERL}$ variants of Slo1 were provided by Dr. Min Li of John Hopkins University (Baltimore, MD) (Kim et al., 2007b; Ma et al., 2007). These constructs are based on mouse sequences. Constructs encoding HA-tagged Short-QEERL and Short-VEDEC were obtained by PCR using Myc-tagged $Slo1_{QEERL}$ as the template for the following paired primers: 5′-ATGGATGCGCTCATCATACCGGTGACC-3′/5′-TGCGCCCGCTCAAAGCCGCTCTTCCT-3′ (Short-QEERL); and 5′-ATGGATGCGCTCATCATACCGGTGACC-3′/5′-TCAACATTCATCT-TCAACCACGTACTTCTG-3′ (Short-VEDEC). The constructs encoding Long-VEDEC and Long-QEERL were PCR-amplified by using the Myc-tagged $Slo1_{VEDEC}$ as a template with the following paired primers: 5′-GGTACCATGGATGCGCTCATCATACCGGTG-3′/5′-TCAACATTCA-TCTTCAACTTCTCTGATTG-3′ (to produce Long-VEDEC); and 5′-GG-TACCATGGATGCGCTCATCATACCGGTG-3′/5-‘TCAAAGCCGCTC-TTCCTGTTCTCTGATTGGAGG-3′ (to produce Long-QEERL).

The PCR products were ligated into pCR2.1 (Invitrogen). After digestion of this plasmid with KpnI and NotI, the Slo1 variants were subcloned into pCMV-HA (Clontech, Mountain View, CA). The identity of these constructs was confirmed by sequencing.

Cell Culture and Transfection. Human embryonic kidney (HEK) 293T cells were grown in Dulbecco's modified Eagle's medium (Invitrogen, Carlsbad, CA) containing heat-inactivated 10% fetal bovine serum and penicillin/streptomycin (Invitrogen) at 37°C in a 5% CO_2 incubator. Cells were transiently transfected for 24 to 48 h using Lipofectamine 2000 (Invitrogen) in serum-reduced medium (OPTI-MEM; Invitrogen) following the manufacturer's instructions. An immortalized mouse podocyte cell line provided by Dr. Peter Mundel (University of Miami, Miami, FL) was grown in RPMI 1640 with 10% fetal bovine serum supplemented with 10 U/ml interferon-γ at 33°C in a 5% CO_2 incubator. Differentiation of these cells was induced by removing interferon-γ and switching to 37°C in a 5% CO_2 incubator for 14 days as described previously (Kim et al., 2008, 2009).

Cell-Surface Biotinylation, Coimmunoprecipitation, and Immunoblot Analysis. Cell-surface biotinylation was carried out by labeling cells with 1 mg/ml EZ-Link sulfo-*N*-hydroxysuccinimide-biotin reagent (Thermo Fisher Scientific, Waltham, MA) in PBS (137 mM NaCl, 10 mM $NaPO_4$, and 2.7 mM KCl, pH 7.4) at 4°C with gentle shaking for 1.5 h. Labeled cells were then incubated in cold PBS containing 100 mM glycine for an additional 20 min at 4°C to stop the reaction. Cells were lysed in PBS containing 0.5% Triton X-100 and a cocktail of protease inhibitors (both from Sigma-Aldrich, St. Louis, MO). Cell lysates were cleared by centrifugation, the supernatants were collected, and a portion of the supernatants was reserved for determination of the total expression of Slo1. The biotinylated proteins from the cell surface were recovered from the remainder of the lysates by incubating with immobilized streptavidin-agarose beads (Thermo Fisher Scientific) at 4°C for 2 h. Beads were washed in PBS and collected by centrifugation and then boiled in 5× Laemmli buffer (50% glycerol, 10% SDS, 10% 2-mercaptoethanol, Tris 50 mM, and 0.02% bromphenol blue).

For immunoprecipitation, cells were lysed, and supernatants were collected as described above. Cell lysates containing 500 mg of total proteins were incubated in the presence of mouse anti-Myc (9B11; Cell Signaling Technology, Danvers, MA) or anti-HA antibodies (6E2; Cell Signaling Technology) at 4°C. After 4 h of incubation, protein A/G agarose beads (Santa Cruz Biotechnology, Santa Cruz, CA) were added to the lysates, which were kept at 4°C for another 16 h with gentle shaking. Beads were extensively washed in PBS, collected by centrifugation, and boiled in Laemmli buffer as described above. Samples were separated by 10% SDS-polyacrylamide gel electrophoresis and proteins were transferred to nitrocellulose paper followed by blocking in 5% nonfat dried milk dissolved in Tris-buffered saline/Tween 20 buffer (10 mM Tris, 150 mM NaCl, and 0.1% Tween 20, pH 7.4). Slo1 proteins were detected by various primary antibodies, including mouse anti-Myc, mouse anti-HA, or rabbit anti-Slo1 (Alomone Labs Ltd., Jerusalem, Israel), as indicated. Horseradish peroxidase (HRP)-conjugated secondary antibodies (Cell Signaling Technology) and SuperSignal West Pico Chemiluminescent Substrate (Thermo Fisher Scientific) were used to visualize immunoreactive bands on autoradiography film. Results were scanned and processed by the National Institutes of Health's

ImageJ software (http://rsbweb.nih.gov/ij/) to determine the intensities of signals.

Electrophysiology and Data Analysis. All recordings were made at room temperature (22°C). Electrophysiological data were digitized and stored for offline analysis using PClamp software (Molecular Devices, Sunnyvale, CA). Whole-cell and inside-out patch recordings were performed in podocytes and HEK293T cells transiently expressing different Slo1 constructs using standard methods described in detail previously (Kim et al., 2007b, 2008, 2009; Zou et al., 2008). For whole-cell recordings from HEK293T cells, the bath solution contained 150 mM NaCl, 0.08 mM KCl, 0.8 mM $MaCl_2$, 5.4 mM $CaCl_2$, 10 mM glucose, and 10 mM HEPES, and the pH was adjusted to 7.4 with NaOH. The pipette solution contained 145 mM NaCl, 2 mM KCl, 6.2 mM $MgCl_2$, 5 μM $CaCl_2$, 10 mM HEPES, and 5 mM *N*-(2-hydroxyethyl)-EDTA (HEDTA), pH 7.2. The free Ca^{2+} concentration in this solution was adjusted to 5 μM as determined using an Orion 97–20 calcium electrode (Thermo Fisher Scientific). Because HEK293T cells do not express endogenous voltage-activated Ca^{2+} channels, the pipette solution was designed to provide sufficient Ca^{2+} to activate BK_{Ca} channels, whereas the reduced K^+ concentrations in bath and pipette salines ensured that macroscopic currents were small enough to avoid saturation of the patch-clamp amplifier. For measurements of whole-cell currents conducted by endogenous BK_{Ca} channels in mouse podocytes, the bath solution contained 150 mM NaCl, 5.4 mM KCl, 0.8 mM $MgCl_2$, 5.4 mM $CaCl_2$, and 10 mM HEPES, pH 7.4. Pipette solutions contained 10 mM NaCl, 125 mM KCl, 6.2 mM $MgCl_2$, and 10 mM HEPES, pH 7.2, and 5 μM free Ca^{2+} buffered with 10 mM HEDTA, as determined with the calcium electrode. For whole-cell recordings, currents were evoked by a series of depolarizing steps from a holding potential of −60 mV. For inside-out patch recordings of pseudomacroscopic currents from HEK293T cells, fire-polished glass micropipettes were filled with a solution containing 140 mM KCl, 1.2 mM $MgCl_2$, 14 mM glucose, and 10 mM HEPES, pH 7.2, and had resistances of 2 to 5 MΩ after filling. Bath solutions contained 140 mM KCl, 1.2 mM $MgCl_2$, 14 mM glucose, and 10 mM HEPES, pH 7.2, and no added Ca^{2+} plus 10 mM EGTA, or 10 μM free Ca^{2+} buffered with 10 mM HEDTA. Currents were evoked by a series of 150-ms depolarizing steps from a holding potential of −80 mV. Activation curves were fitted to the Boltzmann function as described previously (Zou et al., 2008).

VEDEC Peptide Delivery. Penetratin-VEDEC and the octopeptide NH_2-IREVEDEC-COOH (IREVEDEC) were custom-synthesized using a commercial service (Peptide 2.0 Inc., Chantilly, VA). Penetratin peptide (used as a control for Penetratin-VEDEC) was purchased from Innovagen (Lund, Sweden). For cell surface biotinylation assays, HEK293T cells in six-well tissue culture plates were transiently transfected with Slo1-containing plasmids as described above. After 30 h of incubation, transfected cells were washed with PBS and then incubated with a mixture of IREVEDEC and PULSin protein delivery reagent (Polyplus Transfection, Inc., New York, NY) according to the manufacturer's instructions. This mixture was prepared by diluting 1 μg of IREVEDEC in 200 μl of HEPES buffer, pH 7.4, followed by the addition of 12 μl of PULSin reagent. This mixture was incubated at room temperature for 15 min and then added to transfected cells cultured in 2.8 ml of Dulbecco's modified Eagle's medium per well. The same amount of *R*-phycoerythrin (R-PE) provided by the manufacturer was used with PULSin and added to a separate group of cells for use as a negative control. After 4 h of incubation at 37°C, the medium was replaced with regular culture media and cells were incubated for an additional 12 h, at which point cell surface expression was assayed. To examine the effects of VEDEC peptides on endogenously expressed BK_{Ca} channels, mouse podocytes were grown on coverslips coated with type I collagen. Peptide delivery was performed in two different ways. In the first, we prepared a mixture of 3 μg of IREVEDEC or 3 μg of R-PE in 100 μl of HEPES and added 4 μl of PULSin reagent, and then we added this to cells cultured in 0.4 ml of RPMI 1640 medium. In separate experiments, podocytes were treated with 100 μM penetratin or penetratin-VEDEC in OPTI-MEM for 2 to 3 h at 37°C. Currents through BK_{Ca} channels were then measured using whole-cell recordings as described above.

Endocytosis Assay. HEK293T cells were seeded at 30% confluence in 12 wells 24 h before transfection. Twenty-four hours after transfection, cells heterogeneously expressing Myc-tagged $Slo1_{VEDEC}$ or Myc-tagged $Slo1_{QEERL}$ were placed at 4°C for 20 min to stop trafficking and degradation. Surface Slo1 was labeled with mouse anti-Myc in 4°C medium for 1 h. After an extensive wash with cold media, trafficking was allowed to resume by incubating cells at 37°C for different periods of time. Cells were then fixed in PBS containing 4% paraformaldehyde without being permeabilized. Anti-Myc remaining on the cell surface was detected using HRP-conjugated anti-mouse IgG and then exposed to *FAST* OPD reagents (Sigma-Aldrich) for 3 min with constant shaking, at which time the colorimetric reaction was stopped by adding 3 N HCl for 10 min at room temperature. The supernatant was collected, and the optical absorbance was measured at 492 nm using a Multiskan MCC microplate reader (Thermo Fisher Scientific). The endocytosis time constants (τ) were determined by fitting data to a first-order exponential decay function implemented in Origin software (OriginLab Corp, Northampton, MA).

Immunocytochemistry and Confocal Microscopy. HEK293T cells heterologously coexpressing HA-tagged $Slo1_{VEDEC}$ and Myc-tagged $Slo1_{QEERL}$ were fixed in 4% paraformaldehyde in PBS at room temperature for 10 min. Fixed cells were permeabilized and then blocked with PBS containing 0.5% Triton X-100 and 5% bovine serum albumin (BSA) at 37°C for 1 h. Cells were incubated in PBS containing rabbit anti-Myc (1:250; Millipore, Billerica, MA) and mouse anti-HA (1:250; Cell Signaling Technology) with additions of 0.3% Triton X-100 and 3% BSA for 1 h at 37°C. After three washes in PBS, primary antibodies were probed for 1 h at 37°C with Alexa Fluor 568-conjugated anti-mouse IgG (1:1000; Invitrogen, Carlsbad, CA) and Alexa Fluor 488-conjugated anti-rabbit IgG (1:1000; Invitrogen), which were diluted in PBS containing 0.3% Triton X-100 and 3% BSA. Cells were rinsed and mounted, and images were collected on an Olympus FV-1000 inverted stage confocal microscope using a Plan Apo N 60 × 1.42 numerical aperture oil-immersion objective and processed by FluoView software (Olympus, Tokyo, Japan).

Statistics. All quantitative data are presented as mean ± S.E.M. Electrophysiological data were analyzed by Student's *t* test with $P < 0.05$ considered as significant.

Results

Biochemical Interactions between $Slo1_{VEDEC}$ and $Slo1_{QEERL}$. Functional BK_{Ca} channels are minimally composed of four Slo1 proteins, although auxiliary β-subunits can also be present in endogenously expressed channels. We have observed that the $Slo1_{VEDEC}$ and $Slo1_{QEERL}$ isoforms interact biochemically in a heterologous expression system. To do this, we transiently transfected HEK293T cells with plasmids that encode NH_2-terminal (ectofacial) HA-tagged $Slo1_{QEERL}$ and Myc-tagged $Slo1_{VEDEC}$, and then carried out coimmunoprecipitations using antibodies against the tags. Using immunoblot analysis, we detected both HA and Myc when Slo1 was immunoprecipitated with either anti-Myc (Fig. 1A) or anti-HA (Fig. 1B). Neither tag was detected when the initial immunoprecipitation was carried out with normal mouse IgG. Consistent with these results, we observed partial colocalization of $Slo1_{VEDEC}$ and $Slo1_{QEERL}$ by confocal microscopy of transfected HEK293T cells using antibodies against the Myc and HA tags (Fig. 1C), suggesting that a substantial portion of the Slo1 proteins expressed under these conditions are heteromeric.

Coexpression of $Slo1_{VEDEC}$ Suppresses the Steady-State Surface Expression of $Slo1_{QEERL}$. Previous studies have shown that $Slo1_{QEERL}$ is normally expressed at relatively

high levels on the cell surface, whereas $Slo1_{VEDEC}$ is largely retained in intracellular pools (Kim et al., 2007b,c, 2008, 2009; Ma et al., 2007). To examine the behavior of heteromeric channels, cell-surface biotinylation assays were carried out on HEK293T cells transiently expressing HA-$Slo1_{VEDEC}$ and Myc-$Slo1_{QEERL}$ in different ratios (Fig. 2A). These assays were quantified by densitometry (Fig. 2B). In these experiments, the total amount of Slo1-encoding plasmid transfected into cells was the same in each group, which caused the total amount of Slo1 in the HEK293T cells to be constant as measured by immunoblot

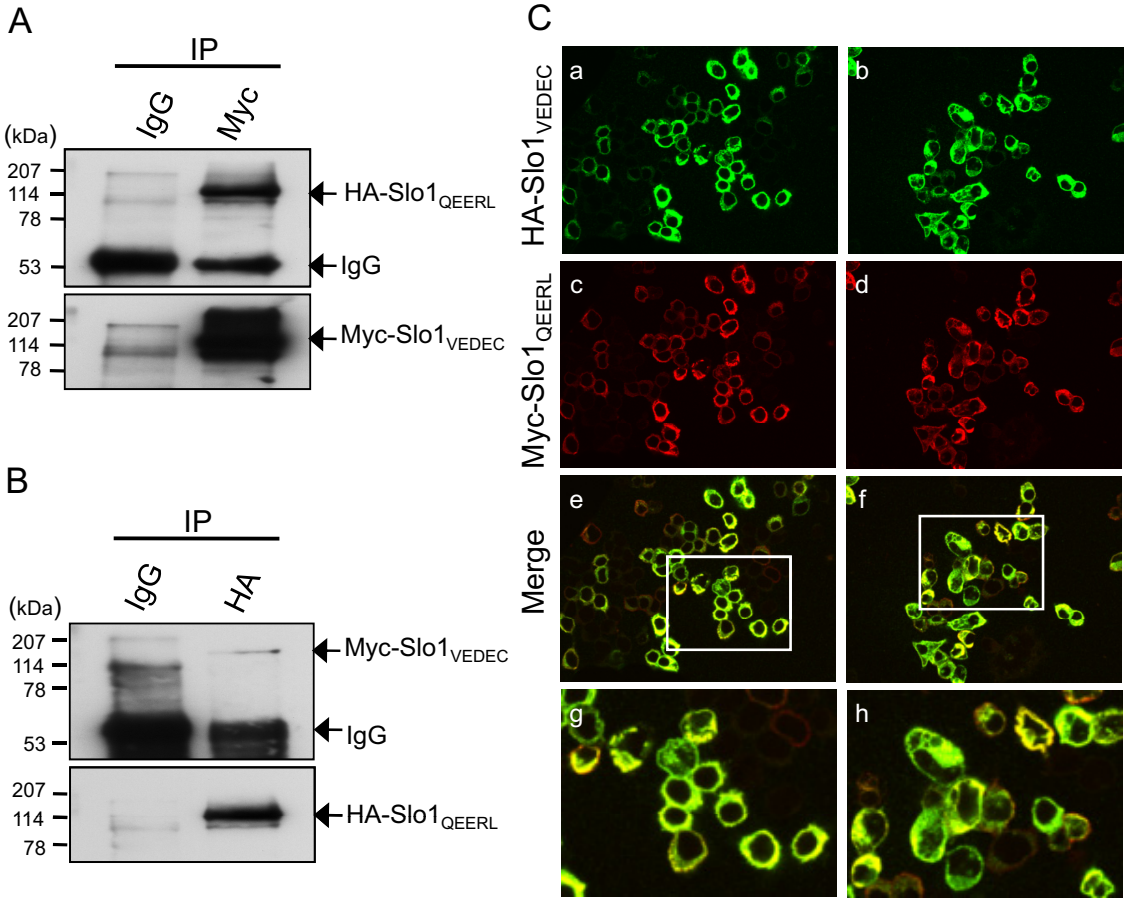

Fig. 1. Coimmunoprecipitation and colocalization of $Slo1_{VEDEC}$ and $Slo1_{QEERL}$ in HEK293T cells. Lysates of HEK293T cells heterologously expressing Myc-tagged $Slo1_{VEDEC}$ and HA-tagged $Slo1_{QEERL}$ were immunoprecipitated with either mouse anti-Myc (A) or anti-HA antibodies (B). Normal mouse IgG served as a negative control. The immunoprecipitated Slo1 proteins were detected with anti-HA or anti-Myc as indicated. C, colocalization of HA-tagged $Slo1_{VEDEC}$ and Myc-tagged $Slo1_{QEERL}$ in HEK293T cells visualized by confocal microscopy. $Slo1_{VEDEC}$ was detected with anti-HA (green, a and b), and $Slo1_{QEERL}$ was detected with anti-Myc (red, c and d). Merged signals of $Slo1_{VEDEC}$ and $Slo1_{QEERL}$ are shown in e to h. Boxed regions in e and f are magnified in g and h, respectively. Colocalization in merged images appear as a yellow signal.

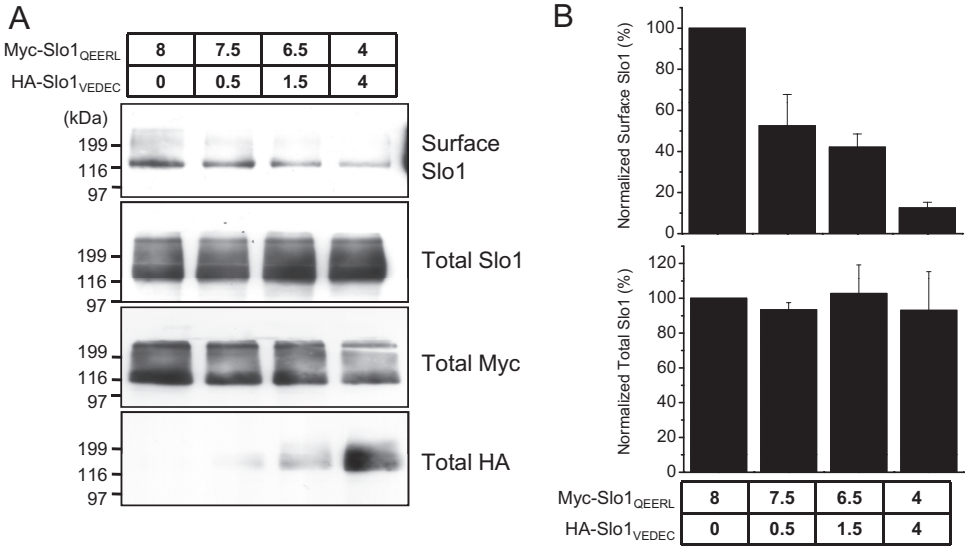

Fig. 2. Coexpression of $Slo1_{VEDEC}$ reduces the surface $Slo1_{QEERL}$ and Slo1 in a dose-dependent manner. HEK293T cells were transiently cotransfected with Myc-tagged $Slo1_{QEERL}$ and HA-tagged $Slo1_{VEDEC}$. The amounts of plasmids used are shown (in micrograms). A, results from representative cell-surface biotinylation assays. B, the total and surface expressions of Slo1 were quantified by densitometry and plotted as mean ± S.E.M. of three experiments.

analysis of total cell lysates using anti-Slo1. Although the total expression of Slo1 proteins remained the same in all groups of cells, the percentage that was on the cell surface was markedly decreased with even a modest increase of total $Slo1_{VEDEC}$ expression relative to $Slo1_{QEERL}$. Thus, a 50% reduction in mean surface expression of Slo1 was observed when only 12.5% of the DNA transfected into the cells encoded $Slo1_{VEDEC}$ and 87.5% encoded $Slo1_{QEERL}$ (Fig. 2B). These data suggest that $Slo1_{VEDEC}$ has a dominant-negative effect on the steady-state expression of Slo1 proteins on the cell surface, probably by trapping heteromeric Slo1 proteins in intracellular compartments. Ma et al. (2007) reached a similar conclusion using a quantitative cell-sorting procedure.

Motif-Swapped Constructs Reveal a Significant Role for the Last Five Residues of Slo1 Splice Variants. The wild-type $Slo1_{VEDEC}$ and the wild-type $Slo1_{QEERL}$ variants that we have studied are identical for their first 1108 residues. The $Slo1_{QEERL}$ form has a short tail that extends 8 residues past the point where the 2 forms diverge, whereas $Slo1_{VEDEC}$ has a long COOH-terminal tail that extends for 61 residues past the point where the isoforms diverge. In principle, a signal that leads to the retention of $Slo1_{VEDEC}$ in intracellular compartments could lie anywhere within the 61-residue VEDEC tail, and Ma et al. (2007) suggested that the entire tail was involved based on deletions of progressively larger portions of the unique components in the $Slo1_{VEDEC}$ tail. However, those sorts of deletions can produce distance effects on the overall structure of the protein and can expose domains for interactions with other proteins that would not normally be available because of steric constraints. Instead, we hypothesized that the essential portion would occur at the very end of the molecules, because with full-length proteins, these residues would be most likely to be exposed for interactions with other molecules. To test this hypothesis, we prepared constructs encoding a series of HA-tagged Slo1 proteins in which the last five residues were switched. These constructs are shown schematically in Fig. 3A and include Slo1 channels with the long tail ending in VEDEC (the wild-type $Slo1_{VEDEC}$, hereafter called Long-VEDEC) and a motif-swapped version that is identical except that it ends in QEERL (hereafter called Long-QEERL). We also prepared Slo1 channels with short COOH-terminal tails that end in QEERL (the wild-type $Slo1_{QEERL}$ form, hereafter referred to as Short-QEERL) and a switched version that ends in VEDEC (Short-VEDEC). All of these constructs are based on mouse sequences. We confirmed these constructs by sequencing and were able to detect their transient expression in HEK293T cells by immunoblot analysis using either anti-HA or anti-Slo1 (Alomone) (Fig. 3B). This antibody did not produce any signal in nontransfected cells (data not shown). We then examined the cell-surface expression of these COOH-terminal wild-type and motif-switched Slo1 variants by means of cell-surface biotinylation assays and whole-cell recordings in HEK293T cells (Figs. 4 and 5). Although Short-QEERL and Short-VEDEC showed similar levels of total expression, the surface expression of Short-VEDEC was markedly reduced compared with that of Short-QEERL (Fig. 4, A and B), although nonlinearities in cell surface biotinylation assays may result in the underestimation of surface expression when signals are faint (Chae et al., 2005a). Consistent with this, the whole-cell current recorded from cells expressing Short-VEDEC was also significantly reduced compared with Short-QEERL (Fig. 4C), although the difference was not as pronounced. Note that in these recordings, the recording electrodes contained a saline in which the free Ca^{2+} was buffered to 5 μM, and currents were evoked by the application of a series of depolarizing voltage steps. We also examined the effects of swapping VEDEC for QEERL at the end of the short Slo1 isoform using inside-out patches in the presence of 10 μM caused a modest rightward shift in the voltage-dependence of activation at these voltages (Fig. 4D). However, this shift cannot account for the marked difference in currents measured at +60 mV, because channels with both COOH-terminal motifs reach maximal activation at that potential. Therefore, the main effect of the motif swap was to change the density of Slo1 channels on the cell surface available for activation. Moreover,

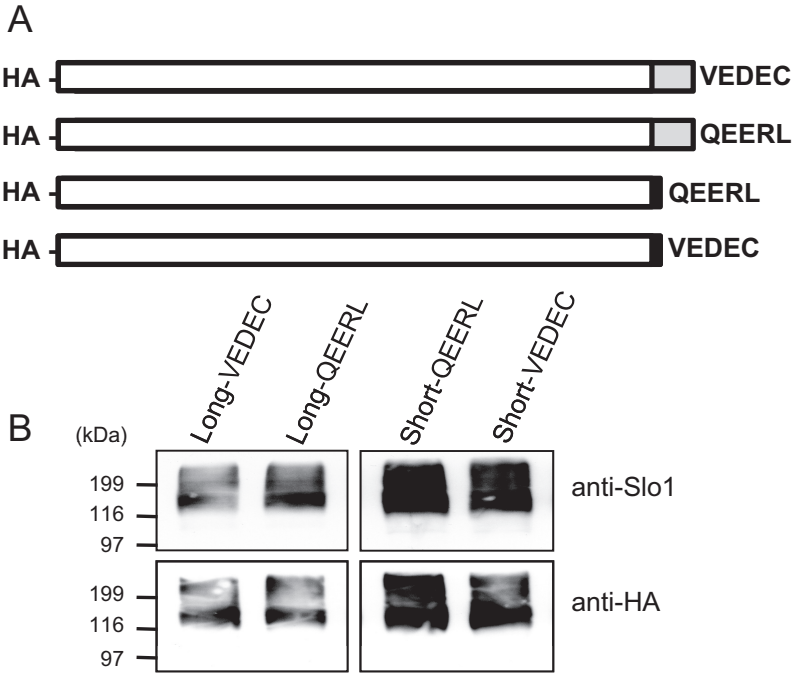

Fig. 3. Motif-swapped constructs of Slo1. A, schematic drawing of motif-swapped Slo1 constructs (not to scale). Top to bottom: Long-VEDEC, Long-QEERL, Short-QEERL, and Short-VEDEC. All of the constructs encode channels with an HA-tag at the NH_2 termini. White boxes represent the identical amino acid sequences in all Slo1 constructs. Gray boxes indicate the VEDEC-specific regions, and the black boxes indicate the QEERL-specific regions. The last five amino acids swapped are shown by letters. B, expression of motif-swapped Slo1 constructs after transient transfection of HEK293T cells determined by immunoblot analysis using the antibodies indicated.

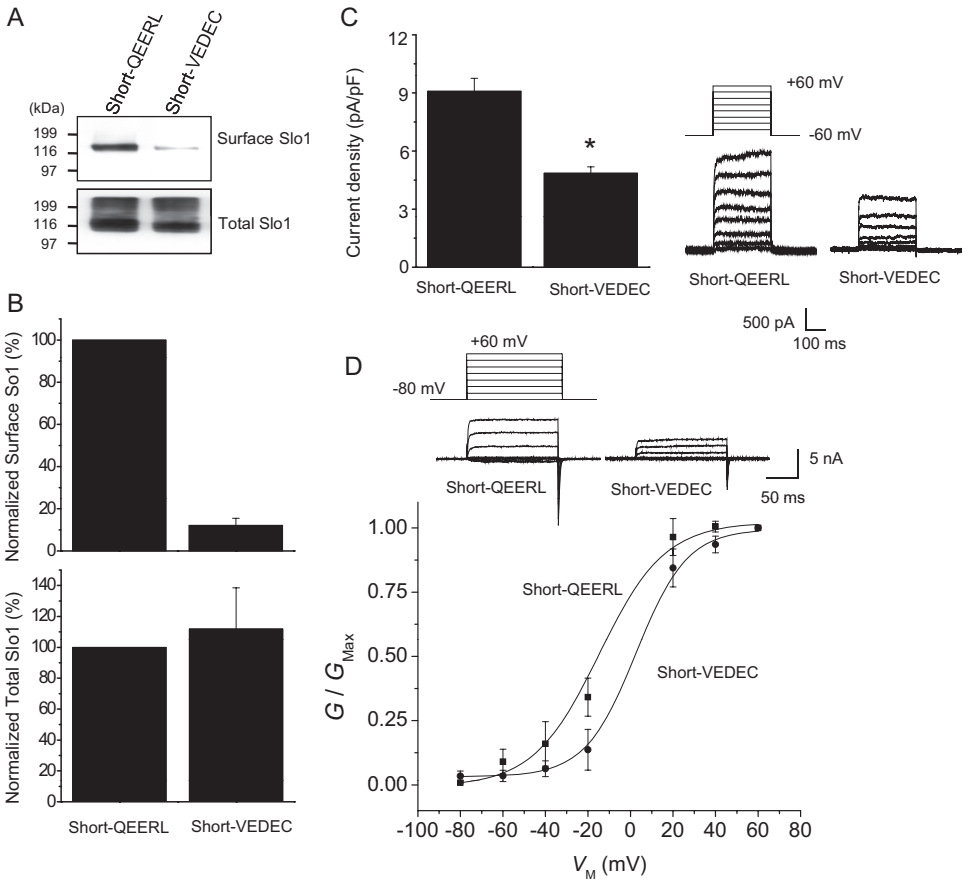

Fig. 4. Short-VEDEC has lower steady-state surface expression than Short-QEERL. A, representative cell-surface biotinylation assays performed in HEK293T cells heterologously expressing Short-QEERL or Short-VEDEC, as indicated. Top, cell surface Slo1; bottom, expression of total Slo1. Signals were obtained by immunoblot analysis using antibodies against the Myc tags. B, summary of densitometric analysis of surface and total expression of Slo1 presented as mean ± S.E.M. from three repetitions of the experiment shown in A. Top, normalized surface Slo1; bottom, total expression of Slo1. C, representative traces of families of currents obtained by whole-cell recording from HEK293T cells expressing Short-QEERL or Short-VEDEC are shown to the right of a bar graph summarizing mean ± S.E.M. of whole-cell current densities evoked by step pulses to +60 mV (n = 34 cells). *, $P < 0.05$. D, voltage-dependence of activation determined in inside-out patches from HEK293T cells expressing Short-QEERL or Short-VEDEC. Recordings were made in symmetrical 140 mM KCl, and bath solutions contained 10 μM free Ca^{2+}. Representative traces are shown above voltage activation curves. Data points are mean ± S.E.M. (n = 11 patches) with superimposed fitted Boltzmann curves. Mean $V_{1/2}$ derived from the Boltzmann fits are −14.3 mV for Short-QEERL and +2.6 mV for Short-VEDEC.

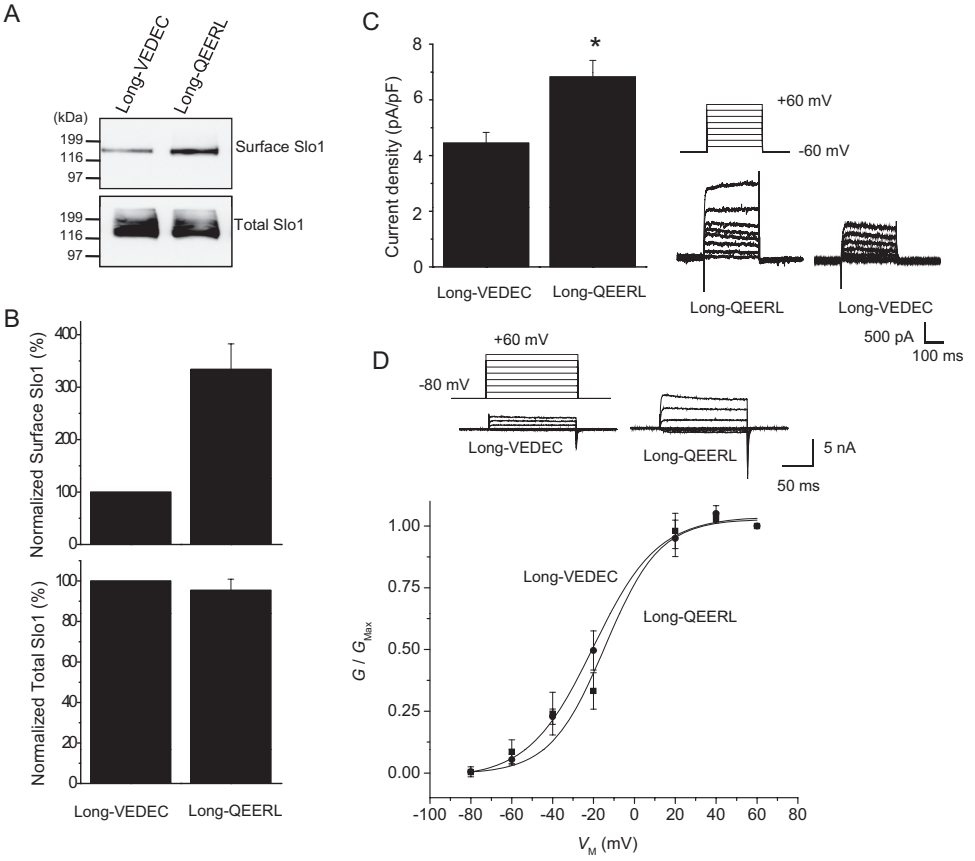

Fig. 5. Long-QEERL has higher surface expression than Long-VEDEC. A, representative cell-surface biotinylation assays performed in HEK293T cells heterologously expressing Long-VEDEC or Long-QEERL, as in the previous figure. B, summary of densitometric analysis of surface and total expression of Slo1 presented as mean ± S.E.M. from three repetitions of the experiment shown in A. C, representative traces of families of currents obtained by whole-cell recording are shown to the right of a bar graph summarizing the mean ± S.E.M. of whole-cell current densities evoked by step pulses to +60 mV (n = 34 cells). *, $P < 0.05$. D, voltage-dependence of activation determined in inside-out patches from HEK293T cells expressing Long-VEDEC or Long-QEERL. Recordings and voltage activation curves were made from 11 patches, as in the previous figure. Mean $V_{1/2}$ values derived from the Boltzmann fits are −14.8 mV for Long-QEERL and −20.1 mV for Long-VEDEC.

we observed a higher surface expression of Long-QEERL compared with Long-VEDEC (Fig. 5, A and B) that was also reflected in qualitatively similar differences in whole-cell current (Fig. 5C). In inside-out patches, we did not see any shift in the voltage-dependence of activation as a result of swapping the terminal pentapeptide motif (Fig. 5D).

In another set of experiments, we examined whether the VEDEC motif can account for dominant-negative effects on Slo1 trafficking that we observed with coexpression of $Slo1_{VEDEC}$. Therefore, we transfected HEK293T cells with combinations of the Short-QEERL and Short-VEDEC constructs (which differ only in the last five residues) and examined surface expression of total Slo1 proteins using the approach already outlined in Fig. 2. We again observed that the presence of the VEDEC motif in only a small portion of the expressed proteins is sufficient to cause robust suppression of Slo1 expression on the cell surface (Fig. 6). These data strongly support the hypothesis that the VEDEC and/or QEERL motifs are involved in regulating the trafficking of Slo1 channels into or out of the cell surface.

VEDEC Peptides Promote the Cell Surface Expression of Slo1. The data on swapped-motif constructs could be interpreted as a positive effect of the QEERL motif on surface expression, a negative effect of the VEDEC motif, or both. In this regard, we have shown previously that cotransfecting full-length $Slo1_{VEDEC}$ channels with a fusion protein composed of green fluorescent protein and the last 42 residues from the COOH terminus of $Slo1_{VEDEC}$ increased the surface expression of full-length $Slo1_{VEDEC}$ and increased whole-cell BK_{Ca} currents in HEK293T cells, whereas green fluorescent protein alone was ineffective (Kim et al., 2007b). For this reason, we hypothesized that the VEDEC motif is sufficient to suppress cell surface expression of Slo1 proteins. If this is the case, introducing short peptides containing the VEDEC motif into cells should also cause an increase in Slo1 expression on the cell surface (by competing with full-length channels for binding to an inhibitory site). In the present study, we used two different approaches to introduce these highly acidic peptides into the cytosol. In the first set of experiments, we synthesized the octopeptide IREVEDEC and delivered it into HEK293T cells expressing full-length $Slo1_{VEDEC}$ or $Slo1_{QEERL}$ using a commercially available proprietary reagent called PULSin (PolyPlus Transfection). A similar amount of R-PE was introduced into control HEK293T cells (which also served to assess the efficiency of the peptide delivery system). We then examined the effect of these treatments on Slo1 using cell-surface biotinylation assays carried out in HEK293T cells heterologously expressing either Myc-$Slo1_{VEDEC}$ or Myc-$Slo1_{QEERL}$. Delivery of IREVEDEC had no effect on the total expression of either Slo1 isoform (Fig. 7). However, the IREVEDEC octopeptide increased the surface expression of $Slo1_{VEDEC}$ compared with that observed in the R-PE control (Fig. 7, A and B). By contrast, IREVEDEC treatment had no effect on the surface expression of $Slo1_{QEERL}$ (Fig. 7, C and D). A similar effect of IREVEDEC was observed in a conditionally immortalized cell line derived from mouse podocytes that endogenously expresses $Slo1_{VEDEC}$ and $Slo1_{QEERL}$ (Kim et al., 2008). These experiments were carried out using whole-cell recordings, and the effect of IREVEDEC on podocyte BK_{Ca} currents was statistically significant (Fig. 8A). Moreover, we observed that IREVEDEC treatment did not alter the activation or deactivation kinetics of macroscopic currents (data not shown). A similar result was obtained in podocytes using a different peptide in which the VEDEC motif was present at the end of the penetratin sequence (Fig. 8B). Penetratin is a 16-residue peptide derived from the third helix of the homeodomain of the Antennapedia protein of *Drosophila melanogaster* (Derossi et al., 1994, 1998). As with several other arginine-rich peptides (Thorén et al., 2003), fusing the penetratin sequence to macromolecules allows them to be taken up by many cell types, although the mechanism whereby this occurs is not well understood. We had a 21-residue peptide synthesized that is composed of the 16 penetratin residues and ending in VEDEC at the COOH terminus (Pene-VEDEC). The 16-residue penetratin peptide (Pene) was used as a control. As with IREVEDEC, we observed that Pene-VEDEC was able to cause a statistically significant increase in whole-cell BK_{Ca} currents in podocytes compared with controls treated with Pene (Fig. 8B). These data support the hypothesis that the VEDEC motif binds to unknown proteins that anchor Slo1 proteins in intracellular compartments. As an aside, note that treatment with Pene and Pene-VEDEC made the membranes of HEK293T cells somewhat fragile and difficult to patch.

Similar Inward Trafficking of $Slo1_{VEDEC}$ and $Slo1_{QEERL}$. The steady-state surface expression of a membrane protein is determined by the rates and balance of movements into and out of

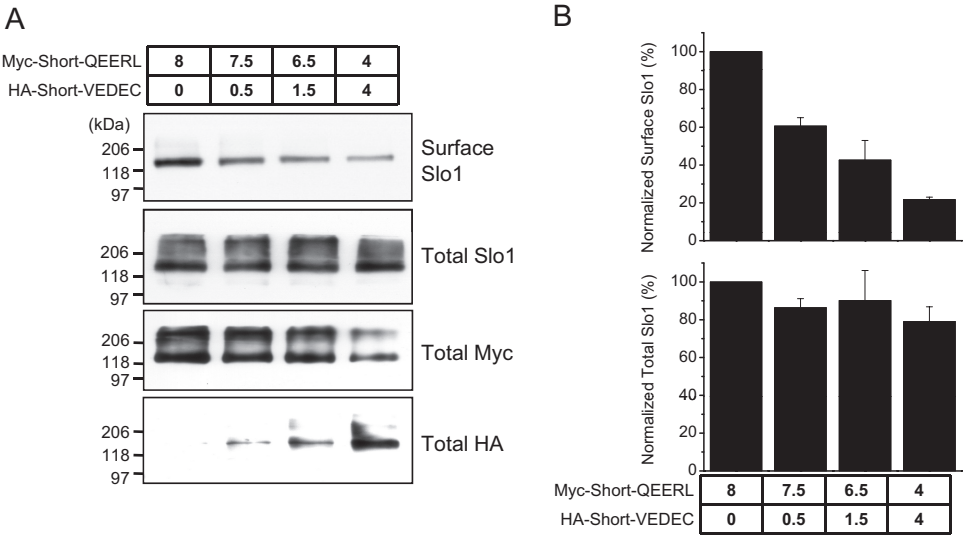

Fig. 6. The VEDEC motif is sufficient to prevent Slo1 from being expressed on the cell surface. HEK293T cells were transiently cotransfected with Myc-tagged Short-QEERL and HA-tagged Short-VEDEC. The amounts of plasmids used are indicated (in micrograms). A, results from representative cell-surface biotinylation assays as well as analyses of total expression of the HA and Myc tags as indicated. Note that total expression of each splice variant is closely related to the amount of each plasmid used in transfection. B, quantification (mean ± S.E.M.) of densitometric analyses of three repetitions of this experiment. Note the reduction of surface expression of Slo1 when even small amounts of Short-VEDEC are present.

the plasma membrane. Whereas the presence of the VEDEC motif in Slo1 reduces constitutive steady-state expression on the cell surface, the available data do not indicate how the VEDEC motif produces this effect. To examine this, HEK293T cells were transiently transfected with either Myc-Slo1$_{QEERL}$ or Myc-Slo1$_{VEDEC}$. After 24 h, the Slo1 proteins on the cell surface were labeled with mouse anti-Myc at 4°C, and inward trafficking was then monitored by bring the cells back to 37°C for different periods of time. The anti-Myc antibodies remaining on the cell surface were labeled with HRP-conjugated anti-mouse IgG and quantified using a colorimetric assay that measured absorbance at 492 nm. In these experiments, the amounts of total expression of Slo1$_{QEERL}$ and Slo1$_{VEDEC}$ determined by immunoblot analysis were indistinguishable (data not shown). Based on this colorometric assay, the total amount of Slo1$_{QEERL}$ on the cell surface was greater than that of Slo1$_{VEDEC}$ at the time at which cells are transferred back to 37°C ($t = 0$), which is consistent with all other methods that we have used to analyze steady-state expression. Both Slo1 isoforms showed a subsequent exponential decrease in cell surface expression over time that reached a new steady state by 60 min, and the rate of internalization was indistinguishable for the two forms (Fig. 9). Specifically, the optical signal for Slo1$_{VEDEC}$ decreased with a time constant of 14.4 ± 3.4 min, and the steady-state decrease of the signal (measured after 60 min) was 0.231 ± 0.065 optical density units (OD_{492}). Signal for Slo1$_{QEERL}$ decreased with a time constant of 15.1 ± 0.9 min, and the steady-state decrease after 60 min was 0.238 ± 0.037 OD_{492} (Fig. 9). These data suggest that the inward trafficking of both splice variants is carried out by similar mechanisms that have indistinguishable capacities and kinetics in HEK293T cells. These data suggest that the effects of the VEDEC motif are exerted primarily on forward trafficking.

Discussion

In the present study, we have shown that two different COOH-terminal splice variants of Slo1, known as Slo1$_{VEDEC}$ and Slo1$_{QEERL}$, are able to form heteromeric channels in a heterologous expression system. This is not surprising because both isoforms contain the tetramerization domain located between Ser6 and Ser7 identified previously (Quirk and Reinhart, 2001); indeed, this domain is present in all Slo1 splice variants. Nevertheless, formation of this particular heteromeric complex has important functional consequences, because we have confirmed an earlier report (Ma et al., 2007) that Slo1$_{VEDEC}$ can exert a dominant-negative effect on the steady-state expression of heteromeric channels to

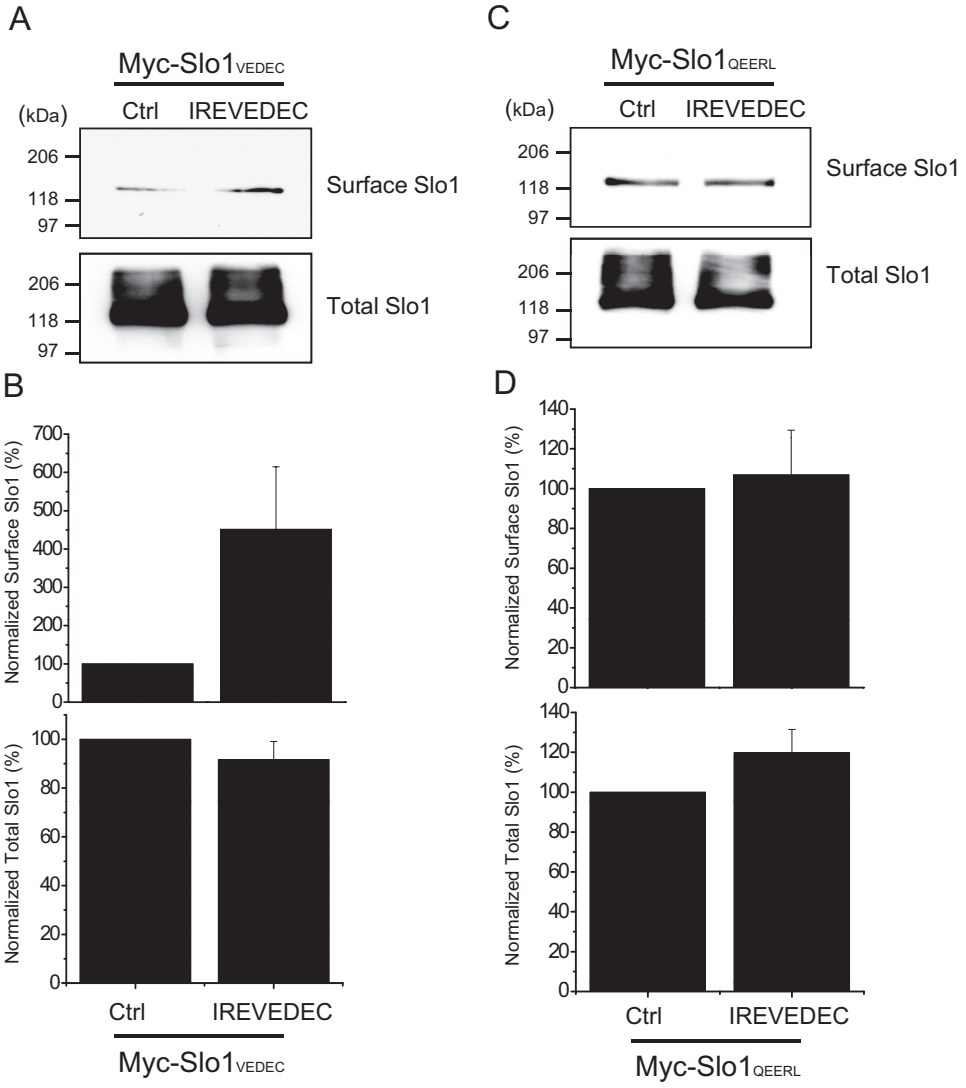

Fig. 7. IREVEDEC peptides increase the surface expression of Slo1$_{VEDEC}$ in HEK293T cells. In these experiments, 1 μg R-PE (Ctrl) or IREVEDEC peptide was delivered into HEK293T cells transiently expressing Slo1$_{VEDEC}$ or Slo1$_{QEERL}$ using PULSin reagent, and cell-surface biotinylation assays were performed 12 h later. Surface and total Slo1$_{VEDEC}$ and Slo1$_{QEERL}$ were detected with anti-Slo1 antibodies. A and C, results from representative cell-surface biotinylation assays. B and D, surface (top) and total (bottom) expression of Slo1 quantified by densitometry and plotted as mean ± S.E.M. from three different experiments compared with R-PE controls.

the cell surface, probably as a result of its binding to an as-yet-unidentified protein that traps the complex in intracellular compartments. This conclusion is supported by the observation that intracellular delivery of two small peptides that contain the VEDEC motif, IREVEDEC and Pene-VEDEC, is able to increase surface expression of heterologously and endogenously expressed Slo1 channels. It bears noting that the VEDEC motif is the only sequence element that these two small peptides have in common.

We and others have shown previously that $Slo1_{QEERL}$ shows robust constitutive expression on the cell surface, whereas $Slo1_{VEDEC}$ is preferentially maintained in intracellular compartments, at least until cells are stimulated with certain growth factors or in the presence of certain Slo1-interacting proteins (Kim et al., 2007a,b). The present data attribute these differences in the behavior of the splice variants to small pentapeptide motifs at the extreme COOH termini of Slo1, a conclusion that is supported by examining the behavior of constructs in which only the last five residues are changed. Thus, Slo1 channels that end in the VEDEC motif have reduced surface expression regardless of whether they end in long or short COOH-terminal tails. Although we cannot entirely exclude that the QEERL motif could play a positive role in cell-surface expression of Slo1, our earlier data suggest that this role must be more limited than that of VEDEC. This is because coexpression of a fusion protein that contains the unique COOH-terminal domains of $Slo1_{QEERL}$ did not produce consistent effects on steady-state surface expression of full-length Slo1, whereas a fusion protein that contained the COOH-terminal domains of $Slo1_{VEDEC}$ behaved identically with the small peptides studied here (Kim et al., 2007b).

Ma et al. (2007) concluded earlier on the basis of sequential deletions of the unique portions of the $Slo1_{VEDEC}$ tail that multiple domains were responsible for reduced surface expression of the $Slo1_{VEDEC}$ isoform. Although the present data cannot exclude that other COOH-terminal motifs play a role in suppressing constitutive surface expression of this variant, they do suggest that the VEDEC motif can account for most of this effect. Differences in experimental design can account for some of the difference in our interpretation; specifically, making substantial deletions can cause alterations in the structure of the entire COOH terminus such that interactions with other proteins could be altered. In addition, deletions could cause other motifs to become sterically available for interactions with other proteins, even though these motifs that may not normally be exposed or in a position to interact in the wild-type forms of these channels. The present strategy of using swapped constructs and short peptide competitors that contain the VEDEC motif minimizes the difficulties in the interpretation of results that arise with deletions.

The present study also provides evidence that $Slo1_{QEERL}$ and $Slo1_{VEDEC}$ are removed from the cell surface of HEK293T cells to a similar extent and by similar kinetics, at least over a period of 1 h. The time course of Slo1 internalization is similar to that of other regulated surface proteins such as GLUT4, aquaporin, and glutamate receptors (Ehlers, 2000; Lin et al., 2000; Huang et al., 2001; Kamsteeg et al., 2006). Unfortunately, we have not been able to reliably measure the rate of forward trafficking under conditions in which this process is kinetically isolated. However, by exclusion, our data suggest that the difference in the constitutive surface expression of $Slo1_{VEDEC}$ and $Slo1_{QEERL}$ is primarily due to differences in their rates of forward trafficking into the plasma membrane.

We have shown previously that $Slo1_{VEDEC}$ and $Slo1_{QEERL}$ are endogenously expressed in the same cell populations, including chick ciliary ganglion neurons (Kim et al., 2007b) and mouse podocytes (Kim et al., 2008). In recent years, our group has examined the role of growth factor-signaling cas-

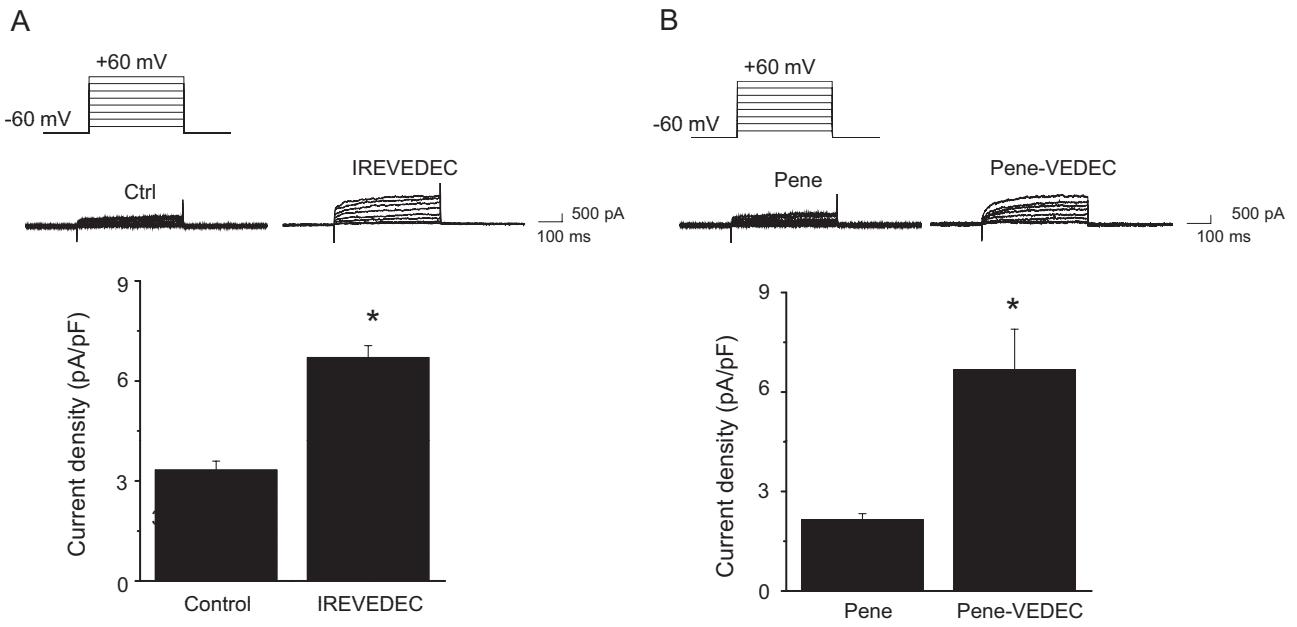

Fig. 8. IREVEDEC and Penetratin-VEDEC peptides increase whole-cell currents in mouse podocytes. Whole-cell recordings were made from differentiated mouse podocytes treated with R-PE or IREVEDEC peptide using PULSin (A) or podocytes treated with penetratin, or penetratin-VEDEC peptides (B). The recording electrode contained 5 μM free Ca^{2+}, and currents were evoked by a series of depolarizing steps from a holding potential of −60 mV. A, top, representative whole-cell currents. Bottom, bar graph shows mean ± S.E.M. of whole-cell currents at +60 mV with n = 33 cells in each group (for IREVEDEC peptides) and 11 cells in each group for penetratin experiments. *, $P < 0.05$.

cades in the regulation of the steady-state surface expression of Slo1 in chick ciliary ganglion neurons (Dryer et al., 2003). In those cells, the surface expression of Slo1 is regulated by at least two different growth factors that signal through phosphoinositide-3 kinase cascades (Lhuillier and Dryer, 2002; Chae and Dryer, 2005; Chae et al., 2005a,b). We have obtained preliminary data that suggest the presence of regulated trafficking of endogenous Slo1 channels in podocytes as well (E. Y. Kim and S. E. Dryer, unpublished observations). It seems likely that a similar type of regulation will occur in any cell type that expresses $Slo1_{VEDEC}$, regardless of which Slo1 variants may be coexpressed.

The mechanism whereby the VEDEC motif traps Slo1 in intracellular compartments is unknown. The VEDEC motif resembles type III PDZ-binding motifs, which are most typically found as the terminal sequence of proteins and have been shown to affect the trafficking and stability of other types of ion channels (Maximov et al., 1999; Okabe et al., 1999; Standley et al., 2000; Duggan et al., 2002). In this regard, we have reported recently that $Slo1_{VEDEC}$ binds to one of the PDZ-domains of a scaffolding protein known as MAGI-1, which causes Slo1 to be sequestered in intracellular compartments in several cell types (Ridgway et al., 2009). Although this would seem to be a promising candidate for a VEDEC-binding protein, we have also observed that MAGI-1 produces a similar effect on $Slo1_{QEERL}$ and on a third COOH-terminal variant known as $Slo1_{EMVYR}$ and can biochemically interact with all three COOH-terminal Slo1 variants (Ridgway et al., 2009). Thus, MAGI-1 is probably not responsible for the different trafficking behaviors of extreme COOH-terminal variants of Slo1, at least not by itself. The present results suggest a mechanism for $Slo1_{VEDEC}$-interacting proteins such as BK_{Ca} β-subunits (Kim et al., 2007c), filamin-A (Kim et al., 2007a), β1 subunits of Na^+-K^+-ATPase (Jha and Dryer, 2009), and nephrin (Kim et al., 2008), which interact with the distal COOH terminus and stimulate surface expression of $Slo1_{VEDEC}$. It is possible that interactions with these proteins sterically inhibit access of the VEDEC motif to other proteins that suppress Slo1 expression on the cell surface. This would provide a basis for dynamic regulation of Slo1 expression based on protein interactions that change over time.

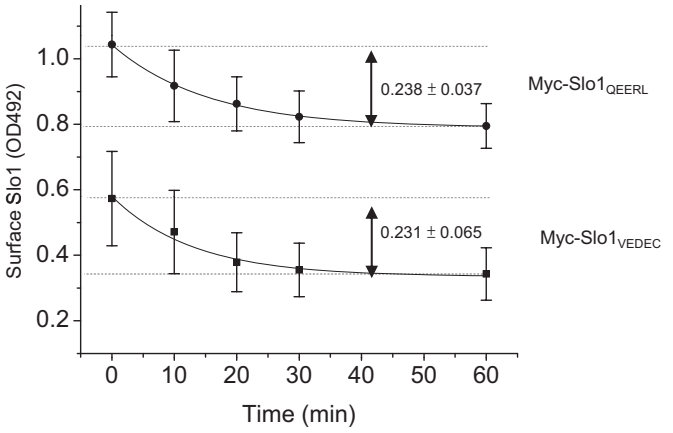

Fig. 9. Time course of $Slo1_{VEDEC}$ and $Slo1_{QEERL}$ removal from the cell surface. Endocytosis assays were carried out by using HEK293T cells heterologously expressing either $Slo1_{VEDEC}$ or $Slo1_{QEERL}$. The expressed channels bear an Myc tag at the extracellular NH_2 terminus, which allowed surface Slo1 on the surface of intact cells to be labeled by anti-Myc at 4°C. Cells were then placed at 37°C for various times to allow trafficking to resume, at which time they were fixed. The amounts of anti-Myc remaining on the cell surface were determined by HRP-conjugated anti-mouse with colorimetric assays at OD_{492}. Data show the time course of OD_{492} (Mean ± S.E.M.) from three different experiments. ■, $Slo1_{VEDEC}$; ●, $Slo1_{QEERL}$. Data are fitted with single-exponential decay functions with time constants of 15.1 ± 0.9 (for $Slo1_{QEERL}$) and 14.4 ± 3.4 min (for $Slo1_{VEDEC}$).

The observation that small VEDEC peptides can stimulate surface expression of Slo1 channels may be of pharmacological use. Slo1 has received considerable interest as a target for therapies for a variety of neurological, cardiovascular, urological, and pulmonary disorders (Nardi and Olesen, 2008). The majority of drug development efforts to date have focused on modulator compounds that stimulate the opening of BK_{Ca} channels that are already in the plasma membrane. The actions of the two short VEDEC peptides suggest a different strategy, namely to inhibit interactions between $Slo1_{VEDEC}$ subunits and proteins that suppress their constitutive trafficking to the cell surface, thereby increasing the density of BK_{Ca} channel complexes at the cell surface. Our data in podocytes suggest that this can lead to an increase in the number of functional endogenously expressed BK_{Ca} channels at the cell surface. The fact that these compounds are short and very acidic peptides would normally be expected to reduce their usefulness as drugs for use in vivo, but because the essential motif is only five residues long, it might be possible to develop more stable and membrane-permeable analogs with a similar mode of action. It is also possible that agents of this type could increase surface BK_{Ca} channels at the expense of other compartments (e.g., mitochondria), in which they may play a completely different physiological role. In this regard, we do not know the nature of the intracellular compartments that harbor $Slo1_{VEDEC}$ subunits, and it may well depend on what cell type is considered. In chick ciliary ganglion neurons, some of it may be associated with cortical actin in post-Golgi pools, at least in some cell types (Chae and Dryer, 2005; Chae et al., 2005b; Zou et al., 2008), whereas other pools are likely to be retained in the endoplasmic reticulum (Lhuillier and Dryer, 2002) and Golgi apparatus (Chae et al., 2005b).

In summary, we have shown that a pentapeptide motif at the extreme COOH terminus of $Slo1_{VEDEC}$ proteins is sufficient to impede constitutive trafficking of complexes containing this motif to the cell surface. Small peptides that contain this motif are able to stimulate the expression of functional BK_{Ca} channels on the cell surface and may suggest new pharmacological strategies for increasing BK_{Ca} function in cells.

Acknowledgments

We are grateful to Dr. Min Li of The Johns Hopkins University (Baltimore, MD) for the Myc-tagged Slo1 expression constructs and to Dr. Peter Mundel of the University of Miami Miller School of Medicine (Miami, FL) for the immortalized podocyte cell line.

References

Beisel KW, Rocha-Sanchez SM, Ziegenbein SJ, Morris KA, Kai C, Kawai J, Carninci P, Hayashizaki Y, and Davis RL (2007) Diversity of Ca^{2+}-activated K^+ channel transcripts in inner ear hair cells. *Gene* **386:**11–23.

Butler A, Tsunoda S, McCobb DP, Wei A, and Salkoff L (1993) mSlo, a complex mouse gene encoding "maxi" calcium-activated potassium channels. *Science* **261:** 221–224.

Chae KS and Dryer SE (2005) The p38 mitogen-activated protein kinase pathway negatively regulates Ca^{2+}-activated K^+ channel trafficking in developing parasympathetic neurons. *J Neurochem* **94:**367–379.

Chae KS, Martin-Caraballo M, Anderson M, and Dryer SE (2005a) Akt activation is necessary for growth factor-induced trafficking of functional K_{Ca} channels in developing parasympathetic neurons. *J Neurophysiol* **93:**1174–1182.

Chae KS, Oh KS, and Dryer SE (2005b) Growth factors mobilize multiple pools of K_{Ca} channels in developing parasympathetic neurons: role of ADP-ribosylation factors and related proteins. *J Neurophysiol* **94:**1597–1605.
Chen L, Tian L, MacDonald SH, McClafferty H, Hammond MS, Huibant JM, Ruth P, Knaus HG, and Shipston MJ (2005) Functionally diverse complement of large conductance calcium- and voltage-activated potassium channel (BK) alpha-subunits generated from a single site of splicing. *J Biol Chem* **280:**33599–33609.
Derossi D, Chassaing G, and Prochiantz A (1998) Trojan peptides: the penetratin system for intracellular delivery. *Trends Cell Biol* **8:**84–87.
Derossi D, Joliot AH, Chassaing G, and Prochiantz A (1994) The third helix of the Antennapedia homeodomain translocates through biological membranes. *J Biol Chem* **269:**10444–10450.
Dryer SE, Lhuillier L, Cameron JS, and Martin-Caraballo M (2003) Expression of K_{Ca} channels in identified populations of developing vertebrate neurons: role of neurotrophic factors and activity. *J Physiol Paris* **97:**49–58.
Duggan A, Garcia-Anoveros J, and Corey DP (2002) The PDZ domain protein PICK1 and the sodium channel BNaC1 interact and localize at mechanosensory terminals of dorsal root ganglion neurons and dendrites of central neurons. *J Biol Chem* **277:**5203–5208.
Ehlers MD (2000) Reinsertion or degradation of AMPA receptors determined by activity-dependent endocytic sorting. *Neuron* **28:**511–525.
Huang J, Imamura T, and Olefsky JM (2001) Insulin can regulate GLUT4 internalization by signaling to Rab5 and the motor protein dynein. *Proc Natl Acad Sci USA* **98:**13084–13089.
Imlach WL, Finch SC, Dunlop J, Meredith AL, Aldrich RW, and Dalziel JE (2008) The molecular mechanism of "ryegrass staggers," a neurological disorder of K^+ channels. *J Pharmacol Exp Ther* **327:**657–664.
Jha S and Dryer SE (2009) The β1 subunit of Na^+/K^+-ATPase interacts with BK_{Ca} channels and affects their steady-state expression on the cell surface. *FEBS Lett* **583:**3109–3114.
Kamsteeg EJ, Hendriks G, Boone M, Konings IB, Oorschot V, van der Sluijs P, Klumperman J, and Deen PM (2006) Short-chain ubiquitination mediates the regulated endocytosis of the aquaporin-2 water channel. *Proc Natl Acad Sci USA* **103:**18344–18349.
Kim EY, Alvarez-Baron CP, and Dryer SE (2009) Canonical transient receptor potential channel (TRPC)3 and TRPC6 associate with large-conductance Ca^{2+}-activated K^+ (BK_{Ca}) channels: role in BK_{Ca} trafficking to the surface of cultured podocytes. *Mol Pharmacol* **75:**466–477.
Kim EY, Choi KJ, and Dryer SE (2008) Nephrin binds to the COOH terminus of a large-conductance Ca^{2+}-activated K^+ channel isoform and regulates its expression on the cell surface. *Am J Physiol Renal Physiol* **295:**F235–F246.
Kim EY, Ridgway LD, and Dryer SE (2007a) Interactions with filamin A stimulate surface expression of large-conductance Ca^{2+}-activated K^+ channels in the absence of direct actin binding. *Mol Pharmacol* **72:**622–630.
Kim EY, Ridgway LD, Zou S, Chiu YH, and Dryer SE (2007b) Alternatively spliced C-terminal domains regulate the surface expression of large conductance calcium-activated potassium channels. *Neuroscience* **146:**1652–1661.
Kim EY, Zou S, Ridgway LD, and Dryer SE (2007c) Beta1-subunits increase surface expression of a large-conductance Ca^{2+}-activated K^+ channel isoform. *J Neurophysiol* **97:**3508–3516.
Kwon SH and Guggino WB (2004) Multiple sequences in the C terminus of MaxiK channels are involved in expression, movement to the cell surface, and apical localization. *Proc Natl Acad Sci USA* **101:**15237–15242.
Lhuillier L and Dryer SE (2002) Developmental regulation of neuronal K_{Ca} channels by TGFβ1: an essential role for PI3 kinase signaling and membrane insertion. *J Neurophysiol* **88:**954–964.
Lin JW, Ju W, Foster K, Lee SH, Ahmadian G, Wyszynski M, Wang YT, and Sheng M (2000) Distinct molecular mechanisms and divergent endocytotic pathways of AMPA receptor internalization. *Nat Neurosci* **3:**1282–1290.
Lu R, Alioua A, Kumar Y, Eghbali M, Stefani E, and Toro L (2006) MaxiK channel partners: physiological impact. *J Physiol* **570:**65–72.
Ma D, Nakata T, Zhang G, Hoshi T, Li M, and Shikano S (2007) Differential trafficking of carboxyl isoforms of Ca^{2+}-gated (Slo1) potassium channels. *FEBS Lett* **581:**1000–1008.
Maximov A, Südhof TC, and Bezprozvanny I (1999) Association of neuronal calcium channels with modular adaptor proteins. *J Biol Chem* **274:**24453–24456.
Meredith AL, Thorneloe KS, Werner ME, Nelson MT, and Aldrich RW (2004) Overactive bladder and incontinence in the absence of the BK large conductance Ca^{2+}-activated K^+ channel. *J Biol Chem* **279:**36746–36752.
Nardi A and Olesen SP (2008) BK channel modulators: a comprehensive overview. *Curr Med Chem* **15:**1126–1146.
Okabe S, Miwa A, and Okado H (1999) Alternative splicing of the C-terminal domain regulates cell surface expression of the NMDA receptor NR1 subunit. *J Neurosci* **19:**7781–7792.
Pietrzykowski AZ, Friesen RM, Martin GE, Puig SI, Nowak CL, Wynne PM, Siegelmann HT, and Treistman SN (2008) Posttranscriptional regulation of BK channel splice variant stability by miR-9 underlies neuroadaptation to alcohol. *Neuron* **59:**274–287.
Quirk JC and Reinhart PH (2001) Identification of a novel tetramerization domain in large conductance K(ca) channels. *Neuron* **32:**13–23.
Ridgway LD, Kim EY, and Dryer SE (2009) MAGI-1 interacts with Slo1 channel proteins and suppresses Slo1 expression on the cell surface. *Am J Physiol Cell Physiol* **297:**C55–C65.
Rüttiger L, Sausbier M, Zimmermann U, Winter H, Braig C, Engel J, Knirsch M, Arntz C, Langer P, Hirt B, et al. (2004) Deletion of the Ca^{2+}-activated potassium (BK) alpha-subunit but not the BKbeta1-subunit leads to progressive hearing loss. *Proc Natl Acad Sci USA* **101:**12922–12927.
Sausbier M, Hu H, Arntz C, Feil S, Kamm S, Adelsberger H, Sausbier U, Sailer CA, Feil R, Hofmann F, et al. (2004) Cerebellar ataxia and Purkinje cell dysfunction caused by Ca^{2+}-activated K^+ channel deficiency. *Proc Natl Acad Sci USA* **101:**9474–9478.
Shen KZ, Lagrutta A, Davies NW, Standen NB, Adelman JP, and North RA (1994) Tetraethylammonium block of Slowpoke calcium-activated potassium channels expressed in *Xenopus* oocytes: evidence for tetrameric channel formation. *Pflugers Arch* **426:**440–445.
Shipston MJ (2001) Alternative splicing of potassium channels: a dynamic switch of cellular excitability. *Trends Cell Biol* **11:**353–358.
Standley S, Roche KW, McCallum J, Sans N, and Wenthold RJ (2000) PDZ domain suppression of an ER retention signal in NMDA receptor NR1 splice variants. *Neuron* **28:**887–898.
Thorén PE, Persson D, Isakson P, Goksör M, Onfelt A, and Nordén B (2003) Uptake of analogs of penetratin, Tat(48–60) and oligoarginine in live cells. *Biochem Biophys Res Commun* **307:**100–107.
Tseng-Crank J, Foster CD, Krause JD, Mertz R, Godinot N, DiChiara TJ, and Reinhart PH (1994) Cloning, expression, and distribution of functionally distinct Ca^{2+}-activated K^+ channel isoforms from human brain. *Neuron* **13:**1315–1330.
Wang SX, Ikeda M, and Guggino WB (2003) The cytoplasmic tail of large conductance, voltage- and Ca^{2+}-activated K^+ (MaxiK) channel is necessary for its cell surface expression. *J Biol Chem* **278:**2713–2722.
Xie J and McCobb DP (1998) Control of alternative splicing of potassium channels by stress hormones. *Science* **280:**443–446.
Zarei MM, Eghbali M, Alioua A, Song M, Knaus HG, Stefani E, and Toro L (2004) An endoplasmic reticulum trafficking signal prevents surface expression of a voltage- and Ca^{2+}-activated K^+ channel splice variant. *Proc Natl Acad Sci USA* **101:**10072–10077.
Zou S, Jha S, Kim EY, and Dryer SE (2008) A novel actin-binding domain on Slo1 calcium-activated potassium channels is necessary for their expression in the plasma membrane. *Mol Pharmacol* **73:**359–368.

Address correspondence to: Dr. Stuart E. Dryer, Department of Biology and Biochemistry, University of Houston, 4800 Calhoun, Houston, TX 77204-5001. E-mail: sdryer@uh.edu